Eur Biophys J (2006) 35: 410–423
DOI 10.1007/s00249-006-0048-8

ARTICLE

Victor V. Skakun · Eugene G. Novikov
Vladimir V. Apanasovich · Hans J. Tanke
André M. Deelder · Oleg A. Mayboroda

Initial guesses generation for fluorescence intensity distribution analysis

Received: 6 October 2005 / Revised: 9 January 2006 / Accepted: 19 January 2006 / Published online: 28 March 2006

Abstract The growing number of applications of Fluorescence Intensity Distribution Analysis (FIDA) demands for new approaches in data processing, aiming at increased speed and robustness. Iterative algorithms of parameter estimation, although proven to be universal and accurate, require some initial guesses (IG) of the unknown parameters. An essential component of any data processing technology, IG become especially important in case of FIDA, since even with apparently reasonable, and physically admissible but randomly chosen IG, the iterative procedure may converge to situations where the FIDA model cannot be evaluated correctly. In the present work we introduce an approach for IG generation in FIDA experiments based on the method of moments. IG are generated for the sample parameters: brightness, concentration, and for the parameters related to experimental set-up: background, observation volume profile. A number of analytical simplifications were introduced in order to increase the accuracy and robustness of the numerical algorithms. The performance of the developed method has been tested on number of simulations and experimental data. Iterative fitting with generated IG proved to be more robust and at least five times faster than with an arbitrarily chosen IG. Applicability of the proposed method for quick estimation of brightness and concentrations is discussed.

V. V. Skakun · A. M. Deelder · O. A. Mayboroda (✉)
Department of Parasitology, Leiden University Medical Centre, Leiden, The Netherlands
E-mail: O.A.Mayboroda@lumc.nl

E. G. Novikov
Service Bioinformatique, Institut CURIE, Paris, France

V. V. Apanasovich · V. V. Skakun
Department of Systems Analysis, Belarusian State University, Minsk, Belarus

H. J. Tanke
Department of Molecular Cell Biology, Leiden University Medical Centre, Leiden, The Netherlands

Keywords Fluorescence intensity distribution analysis · Photon counting histogram · Fluorescence cumulants analysis · Fluorescence fluctuation spectroscopy · Fluorescence correlation spectroscopy · Data analysis · Method of moments

Introduction

Fluorescence fluctuation spectroscopy (FFS) is a group of methods capable of using small spontaneous variations of the fluorescence intensity as a source of information about physico-chemical parameters of the measured sample. One of the best-known realizations of FFS is Fluorescence Correlation Spectroscopy (FCS) (Magde et al. 1972, 1974; Elson and Magde 1974; Rigler et al. 1993; Hess et al. 2002). In FCS, the autocorrelation function of fluorescence intensity is used to obtain information about the number and average residence time of the molecules in the observation volume. Although FCS is a robust and reliable method, it has some limitations, especially when questions on interaction between molecules are raised. If two species of molecules have to be differentiated on the basis of autocorrelation function analysis, the difference in molecular weight has to be at least a factor of 5–8, depending on the type of molecules, the solvent and the fluorescence intensity (Meseth et al. 1999). The second major limitation of FCS is its inability to evaluate correctly cases where molecules have different molecular brightness (e.g. in the case of proteins dimerization) (Kask et al. 2002).

To address these shortcomings of FCS another method, known as Fluorescence Intensity Distribution Analysis (FIDA) (Kask et al. 1999) or Photon Count Histogram (PCH) (Chen et al. 1999) has been proposed: an acquired trace of photon arrival times is divided in short time intervals (time window) and a frequency histogram of photon numbers a photon counting distribution (PCD) detected within a given time window is constructed and fitted by the theoretical model, revealing the number of particles and their average molecular

brightness value. Thus, FIDA differentiates species on the basis of their molecular brightness rather than molecular weight. It has been shown that even without detailed knowledge of the physico-chemical conditions of the sample FIDA is capable of resolving brightness ratio's of two from a single measurement (Müller et al. 2000; Kask et al. 2002) and therefore experimental evaluation of dimerization or aggregation phenomena can be addressed. The feasibility of FIDA has also become evident from a number of extensions of the method, such as 2D-FIDA (Kask et al. 2000), FIMDA for the simultaneous determination of diffusion coefficients and specific brightness values (Palo et al. 2000), and FILDA combining FIDA and fluorescence lifetime measurements (Palo et al. 2002).

Data analysis of both FIDA and PCH implies fitting a theoretical model to the experimental PCD (to avoid misunderstanding, we will refer here to the PCD as a name of measured statistical characteristic and FIDA and PCH as names of analysis methods). In general, iterative methods, in which a new set of parameters is generated on the basis of available initial guesses (IG), are used (Johnson and Faunt 1992). If IG are in close proximity to the unknown parameters, they can significantly increase the efficiency and accuracy of the fit, and if the target criterion surface has a complex shape with many local minima, the possibility to reach global minima directly depends on the quality of the IG. Moreover, for a certain combination of parameters the FIDA model cannot be numerically evaluated (leading to division by zero, numerical overflow, etc.). And last, but not the least, implementation of FIDA implies application of Fast Fourier Transformation (FFT): the theoretical model is initially calculated in the frequency domain and is then converted into PCD. Since the frequency domain is always restricted, this leads to distortions of the resulting PCD. Ten times increase of concentration or brightness often moves PCD away from the model domain.

There are also practical reasons to pay special attention to IG generation for the FIDA model. FIDA was proposed as a possible platform for development of high throughput screening methods (Kask et al. 1999, 2000; Palo et al. 2000, 2002). Indeed, the selectivity of fluorescence technologies and their sensitivity may well be used for high throughput screening, but also demand implementation of fast and reliable parameter minimization algorithms, which, in turn, require correct IG to decrease the number of iterations and to speed up data processing. It is also important that a reliable algorithm of IG generation reduces user participation and thereby leads to a more standardized procedure.

Here we propose a fast and effective method of IG generation for the FIDA model. It is based on the statistical method of moments and will simplify, speed up and increase the numerical and statistical robustness of FIDA analysis especially in a situation where multiple samples have to be quickly evaluated as is for instance the case in high throughput screening. The developed method of IG generation can be also used independently for quick estimation of brightness and concentrations.

Theory

Method of moments

Method of moments (Korn and Korn 1968) is widely used in statistics to estimate parameters for any probability distribution, for which the necessary amount of moments can be generated. According to this method theoretically obtained moments $M_k = M_k(\eta_1, \eta_2, ..., \eta_m)$ are equalized to the experimentally obtained ones $\tilde{M}_k$:

$$M_k(\eta_1, \eta_2, \ldots, \eta_m) = \tilde{M}_k, \; k = 1, 2, \ldots, m, \tag{1}$$

where η_1, η_2, ..., η_m is a set of unknown parameters. The solution of system of (1) yields the estimations for η_1, η_2, ..., η_m.

Moments of probability distribution

Theoretical moments are defined via probability distribution $P(n)$ (Korn and Korn 1968).

$$M_k = \langle n^k \rangle = \sum_{n=1}^{\infty} n^k P(n). \tag{2}$$

Method of moments can also be reformulated in terms of factorial moments F_k or factorial cumulants K_k that may lead to considerable simplification in further mathematical derivations. To calculate theoretical factorial moments and factorial cumulants it is convenient to introduce the concept of generating function. The generating function is given by (Korn and Korn 1968).

$$G(\xi) = \sum_{n=0}^{\infty} \xi^n P(n), \tag{3}$$

where ξ is trial variable, and the factorial moments and factorial cumulants can be calculated as generating function derivatives

$$F_k = \left. \frac{\mathrm{d}^k G(\xi)}{\mathrm{d}\xi^k} \right|_{\xi=1}, \tag{4}$$

$$K_k = \left. \frac{\mathrm{d}^k \ln\, G(\xi)}{\mathrm{d}\xi^k} \right|_{\xi=1}, \tag{5}$$

respectively. Experimental moments are defined as

$$\tilde{M}_k = \langle n^k \rangle = \sum_{n=1}^{m} n^k P^*(n), \tag{6}$$

where $P^*(n)$ is the normalized PCD, i.e. the measured probability to detect n photons within a counting time interval T, the angular brackets indicate averaging over the set of probabilities $P^*(n)$, $n = 0,1, ..., m$. Experimental

factorial moments and factorial cumulants are defined as:

$$\tilde{F}_k = <n(n-1)\dots(n-k+1)> = \sum_{n=k}^{m} n(n-1)\dots(n-k+1)P^*(n), \quad (7)$$

and

$$\tilde{K}_k = \tilde{F}_k - \sum_{i=1}^{k-1}\left(\frac{k-1}{i}\right)\tilde{K}_{k-i}\tilde{F}_i, \text{where}\left(\frac{k-1}{i}\right) = C_{k-1}^{i} = \frac{(k-1)!}{i!(k-i-1)!}. \quad (8)$$

For instance, the first four factorial moments read

$$\begin{aligned} F_1 &= \langle n\rangle = M_1,\\ F_2 &= \langle n(n-1)\rangle = \langle n^2\rangle - \langle n\rangle = M_2 - M_1,\\ F_3 &= \langle n(n-1)(n-2)\rangle = \langle n^3\rangle - 3\langle n^2\rangle + 2\langle n\rangle\\ &= M_3 - 3M_2 + 2M_1,\\ F_4 &= \langle n(n-1)(n-2)(n-3)\rangle\\ &= \langle n^4\rangle - 6\langle n^3\rangle + 11\langle n^2\rangle - 6\langle n\rangle\\ &= M_4 - 6M_3 + 11M_2 - 6M_1 \end{aligned}$$

and the corresponding factorial cumulants take the form

$$\begin{aligned} K_1 &= F_1 = M_1,\\ K_2 &= F_2 - K_1F_1 = F_2 - F_1^2,\\ K_3 &= F_3 - 2K_2F_1 - K_1F_2 = F_3 - 3F_1F_2 + 2F_1^3,\\ K_4 &= F_4 - 3K_3F_1 - 3K_2F_2 - K_1F_3 = F_4 + 12F_1^2F_2 - 4F_1F_3\\ &\quad - 3F_2^2 - 6F_1^4. \end{aligned}$$

Analysis of fluorescence fluctuation moments

Introducing the method of moments to the field of FFS Qian and Elson proposed the following system of equations (Qian and Elson 1990a, 1990b):

$$\begin{cases} \langle\Phi\rangle = \chi_1\sum_i q_i c_i\\ \langle\Delta\Phi^2\rangle = \chi_2\sum_i q_i^2 c_i\\ \langle\Delta\Phi^3\rangle = \chi_3\sum_i q_i^3 c_i\\ \langle\Delta\Phi^4\rangle - 3\langle\Delta\Phi^2\rangle^2 = \chi_4\sum_i q_i^4 c_i \end{cases}, \quad (9)$$

where $\langle \Delta\ \Phi\ ^k\ \rangle$ are central moments of fluorescence intensity of order k, $\chi_k = \int B^k(r)\,\mathrm{d}r$ is an integral over the observation volume, and q_i and c_i are the mean number of photons detected in a time interval and the mean number of particles of ith component in the open observation volume, respectively. System of equations 9 represents the first four cumulants of fluorescence intensity. Using the aggregation process as a model, Qian and Elson have shown that only three first moments are necessary to resolve a two-component mixture (Qian and Elson 1990b).

Moments calculated from fluorescence intensity are not identical to those calculated from photon arrival times: shot noise effects have to be taken into account. For that, the factorial moments of a number of photon counts n (Qian 1990; Qian and Elson 1990a) can be used:

$$\begin{cases} \langle\Phi\rangle = \langle n\rangle\\ \langle\Delta\Phi^2\rangle = \langle\Delta n^2\rangle - \langle n\rangle\\ \langle\Delta\Phi^3\rangle = \langle\Delta n^3\rangle - 3\langle\Delta n^2\rangle + 2\langle n\rangle\\ \langle\Delta\Phi^4\rangle - 3\langle\Delta\Phi^2\rangle^2 = \langle\Delta n^4\rangle - 6\langle\Delta n^3\rangle + 11\langle\Delta n^2\rangle\\ \qquad\qquad -3\langle\Delta n^2\rangle^2 - 6\langle n\rangle, \end{cases} \quad (10)$$

where $\langle\Delta n^k\ \rangle = \sum_{n=0}^{\infty}\ (n\ -\ \langle n\ \rangle)^k\ P(n)$ are central moments of order k.

The recently introduced Fluorescence Cumulant Analysis (FCA) (Muller 2004) extends Qian and Elson's method to an arbitrary number of cumulants

$$K_k = \chi_k\sum_i c_i q_i^k. \quad (11)$$

Although, Qian and Elson's approach is simple and describes the experimental situation well, it is of little use for IG generation for the FIDA model. FIDA uses a different approximation of observation volume and accounts for the background count rate of detector, and therefore one has to calculate IG for three additional parameters.

Model of fluorescence intensity distribution

The generating function of probability of detecting n photons $P(n)$ emitted by a number of fluorescent molecules situated in an inhomogeneous observation volume V at equilibrium state during counting time interval T can be written as (Evotec Int Patent 1998; Kask et al. 1999)

$$G(\xi) = \exp\left(c\int_V\{\exp[(\xi-1)qTB(r)] - 1\}\mathrm{d}V\right), \quad (12)$$

where c is a concentration expressed in terms of a mean number of molecules in the observation volume, q is a specific brightness of molecules represented by a mean number of photons per counting time interval per molecule, $B(r)$ is brightness profile function, which is the product of excitation intensity and detection efficiency and is a function of spatial coordinates r. It is assumed that the contribution of each single molecule to the recorded photon trace is independent, the diffusion is negligible during the counting time interval T, and effects of saturation and triplet state are neglected.

One of the key features of the approach proposed by Evotec is a flexible model for brightness profile function $B(r)$, allowing an approximation of a broad spectrum of confocal volume shapes

$$\frac{\mathrm{d}V}{\mathrm{d}x} = A_0(x + ax^2 + bx^3), x = \ln\left[\frac{B_0}{B(r)}\right], \tag{13}$$

where A_0, a, b are instrumental parameters and B_0 is the value of $B(r)$ at r equal 0. B_0 and A_0 are calculated from a system of normalization equations:

$$\begin{aligned} &\int_V B(r)\mathrm{d}V = 1, \\ &\int_V B^2(r)\mathrm{d}V = 1. \end{aligned} \tag{14}$$

Equation 12 can be extended for the case where the investigated sample consists of molecules with different brightness characteristics and where the contribution of a background noise to the data is not fully eliminated (Kask et al. 1999)

$$G(\xi) = \exp\left((\xi - 1)\lambda T + \sum_j c_j \int_V \left\{\exp\left[(\xi - 1)q_j TB(r)\right] - 1\right\}\mathrm{d}V\right), \tag{15}$$

where j is an index of a molecular species and λ is the mean background count rate of detector. Replacing ξ by $\mathrm{e}^{i\varphi}$ converts the generating function to the characteristic function. As the probability distribution and its characteristic function are interlaced by the Fourier transform, $P(n)$ can be calculated from (15) using inverse FFT

$$P(n) = \mathrm{FFT}^{-1}(G(\mathrm{e}^{i\varphi})). \tag{16}$$

Materials and methods

Sample preparation

Alexa 488 maleimide was purchased from Molecular Probes (Molecular Probes Europe BV; The Netherlands) and mouse Fab2-Cy2 from Amersham (The Netherlands). A mouse IgG was fluorescently labelled with Alexa 488 according to the manufacturer's recommendation. A detailed overview of production and characterization of monoclonal antibodies used in the present study has been published before (Deelder et al. 1996; Remoortere et al. 2000).

Instrumentation

FCS setup and measurements

All measurements were carried out with a ConfoCor 2 System (Zeiss, Germany) equipped with Zeiss Neofluar (40× 1.2 N.A.) water immersion objective as focusing optics. The 488 nm line of the Argon-ion laser was used for excitation. As a sample carrier glass-bottom 96-well plates (Polyfiltronics, USA) were used. PBS (0.035 M phosphate, 0.15 M NaCl, pH 7.6) was used as a solvent.

Simulation of PCD. PCD has been simulated by the calculation of a noise-free curve and the addition of the proper noise to each point of the calculated curve (Demas 1983). Statistical noise of the experimental PCD can be well characterised by the Binomial distribution:

$$P\{\zeta = l\} = \frac{M!}{l!(M-l)!}p^l(1-p)^{M-l},\ l = 0, 1, 2, \ldots, M, \tag{17}$$

where p is the probability of receiving n photons during bin time T and M is total number of bins. The mean μ and the variance σ^2 of the binomial distribution are given by $\mu = Mp$ and $\sigma^2 = Mp(1-p)$, respectively. Thus, in order to generate each point i of noisy PCD one first has to calculate the theoretical PCD $P(i)$ defined by (15) and (16) and then at each point generate the Binomial random number with given M and $p = P(i)$. Straightforward application of (17) is unpractical for large M, so an approximation has to be used instead. For a typical FFS experiment the measured PCD may vary over several orders of magnitude. For large $MP(i)$ (in practice when $MP(i) > 30$) the normal distribution with mean $MP(i)$ and standard deviation $\sqrt{MP(i)(1-P(i))}$ approximates Binomial distribution well (Korn and Korn 1968) (in order to reproduce real measurements the generated values must be rounded off to the nearest integer). For smaller $MP(i)$, where M is still large and $P(i)$ is relatively small the Poisson approximation with parameter $MP(i)$ may be used (Korn and Korn 1968).

The signal to noise ratio (S/N), defined as $S/N = \mu/\sigma$ (Koppel 1974), is taken usually as an initial parameter for noisy curve simulation. If S/N is taken at the maximum of the simulated curve $p_{\max} = \max_i(P(i))$, this results in

$$S/N = \sqrt{Mp_{\max}/(1-p_{\max})}, \tag{18}$$

and thus

$$M = (S/N)^2(1-p_{\max})\Big/p_{\max}. \tag{19}$$

It is practical to use the number of counts at the maximum ($V_{\max}$) of the simulated curve for S/N estimation. Then, M is given by $M = V_{\max}/p_{\max}$ and consequently $S/N = \sqrt{V_{\max}/(1-p_{\max})}$.

Data analysis

PCD were calculated from ConfoCor2 raw data with FCS Data Processor 1.3 (http://www.SSTCenter.com). A homemade software realization of the FIDA model

was used for analysis of the obtained PCD. The fitting procedure is based on the Marquardt–Levenberg nonlinear least squares algorithm (Marquardt 1963). The goodness of the fit is judged by reduced χ^2 criterion and visual inspection of the weighted residuals. Weight factors are calculated as standard deviations of Binomial distribution given by $\sigma_i = \sqrt{MP^*(i)(1-P^*(i))}$, where M is the total number of bins. Because M is usually large, Binomial distribution is approximated well by normal distribution and therefore the application of reduced χ^2 criterion is justified.

The theoretical distribution $P(n)$ was calculated according to (15) and (16). Integration was performed numerically by Simpson's method with Richardson correction (Lau 1995). Numerical solution of system of nonlinear equations was done by Newton–Raphson method (Press et al. 1992).

Results

Calculation of IG for FIDA by method of moments

According to the method of moments (see Theory) we first calculate the theoretical factorial cumulants of $P(n)$. Substituting (15) into (5) yields

$$\begin{aligned} K_1 &= \lambda T + \sum_j c_j q_j T \int_V B(r) \exp\left[(\xi-1) q_j T B(r)\right] \mathrm{d}V \Big|_{\xi=1} \\ &= \lambda T + \chi_1 \sum_j c_j q_j T \\ K_k &= \chi_k \sum_j c_j q_j^k T^k, \; k = 2, 3, \ldots, \end{aligned} \tag{20}$$

where

$$\chi_k = \int_V B^k(r) \mathrm{d}V. \tag{21}$$

Using the normalization condition from (14) ($\chi_1 = \chi^2 = 1$) we get:

$$\begin{aligned} K_1 &= (\lambda + \sum_j c_j q_j) T \\ K_2 &= \sum_j c_j q_j^2 T^2 \\ K_k &= \chi_k \sum_j c_j q_j^k T^k, \; k = 3, 4, \ldots, \end{aligned} \tag{22}$$

where χ_k can be rewritten in terms of the unknown parameters a and b. Substituting (13) into (21) yields

$$\chi_k = \int_0^\infty (B_0 \mathrm{e}^{-x})^k A_0 (x + a x^2 + b x^3) \mathrm{d}x. \tag{23}$$

From (14) and (23) we get expressions for B_0 and A_0

$$B_0 = 8u/v, \; A_0 = v/8u^2, \tag{24}$$

where

$$u = 2a + 6b + 1 \quad \text{and} \quad v = 2a + 3b + 2. \tag{25}$$

All unknown parameters can be estimated from a system, where theoretical factorial cumulants (22) are equalized to the experimentally obtained ones (8). From practical point of view, however, instability of high order factorial cumulants of PCD may result in divergence of numerical solution. Moreover, systems of nonlinear equations are usually solved by iterative procedure and thus require IG by its own. Therefore let us consider more simple cases leading to solutions without iterative calculations.

IG for one component system

According to the method of moments one has to write one equation for each estimated parameter c, q, λ, a and b. After analytical integration (23) over x and substituting into (22) we arrive at

$$\begin{aligned} K_1 &= (\lambda + cq) T \\ K_2 &= cq^2 T^2 \\ K_3 &= cq^3 T^3 (2a + 2b + 3) \frac{64u}{27v^2} \\ K_4 &= cq^4 T^4 (4a + 3b + 8) \frac{4u^2}{v^3} \\ K_5 &= cq^5 T^5 (10a + 6b + 25) \frac{4096u^3}{625v^4}. \end{aligned} \tag{26}$$

System of nonlinear equations (26) can be solved analytically. From the first two equations we get expressions for q and c

$$q = \frac{K_2}{(K_1 - \lambda T) T} \quad \text{and} \quad c = \frac{(K_1 - \lambda T)^2}{K_2}. \tag{27}$$

Substituting (27) into the three last equations of system 26 yields the system for parameters a and b

$$\frac{(10a + 6b + 25)(2a + 2b + 3)}{(4a + 3b + 8)^2} = \frac{16\,875 K_5 K_3}{16\,384 K_4^2}$$

$$\frac{(2a + 3b + 2)(4a + 3b + 8)}{(2a + 2b + 3)^2} = \frac{1\,024 K_4 K_2}{729 K_3^2}$$

and the expression for λ

$$\lambda = K_1 - \frac{64 K_2^2}{27 K_3} \frac{(2a + 2b + 3)(2a + 6b + 1)}{(2a + 3b + 2)^2}. \tag{29}$$

System 28 can be reduced to the fourth order polynomial (see Appendix 1) with respect to a or b and be solved either numerically, or analytically. If the discriminant of the polynomial is positive, the solution gives

us two real and two complex-conjugate roots (Korn and Korn 1968). One real root (always represented by values $a=-7/2$ and $b=2$) leads to singularity of the model ($c=0$ $q=\infty$, see 27) and must be omitted. Thus, only one combination of parameters is admissible as IG. If the discriminant is negative, four real roots are available. One root is again represented by values $a=-7/2$ and $b=2$ and must be omitted. Three other sets of parameters are meaningful. Multiplicity of the admissible algebraic solutions is probably a consequence of the combination of the observation profile approximation from (13) and the normalization conditions given by (14). This requires careful designing of the procedure for selection of the unique and correct combination of parameters. For example, to select the appropriate set we can either reject unrealistic values, or to accept set of parameters, ensuring the lowest value of χ^2 criterion.

If λ is known (it can be estimated from additional measurements of background signal using the formula $\lambda=K_1/T=\langle n \rangle/T$), system 26 is simplified to four equations. Then, using normalization conditions given by (14), c and q can be estimated from (27) independently from brightness profile parameters a and b. The estimates for a and b are calculated from third and fourths equations of system 26

$$\begin{aligned}\frac{64(2a+6b+1)(2a+2b+3)}{27(2a+3b+2)^2} &= \frac{(K_1-\lambda T)K_3}{K_2^2}=\chi_3\\ \frac{4(2a+6b+1)^2(4a+3b+8)}{(2a+3b+2)^3} &= \frac{(K_1-\lambda T)^2K_4}{K_2^3}=\chi_4.\end{aligned} \tag{30}$$

In general, all χ_k can be calculated from the factorial cumulants

$$\chi_k=\frac{(K_1-\lambda T)^{k-2}K_k}{K_2^{k-1}}. \tag{31}$$

The way of solution of system 30 is equivalent to that of system 28. It can be also reduced to the fourth order polynomial and thus a possibility to get a number of roots remains.

If λ is fixed, then c and q are independent from a and b. So, for any combination of a and b there exists the same set of c and q. All possible combinations of a and b are roots of system 30, which give the same values for observation volume integrals χ_k, so one should get the same PCD for all those combination of parameters. As a consequence, the value of χ^2 criterion should be the same for all those roots. Subsequently setting physically meaningful ranges for parameters might be a more attractive way of selection of roots, than the minimization of χ^2. For further simplification we may assume $\lambda=0$. In that case we get the well known formulas (Chen et al. 1999, 2000, 2002) for c and q

$$q=\frac{K_2}{K_1T}=\frac{\langle\Delta n^2\rangle-\langle n\rangle}{\langle n\rangle T},\ c=\frac{K_1^2}{K_2}=\frac{\langle n\rangle^2}{\langle\Delta n^2\rangle-\langle n\rangle} \tag{32}$$

And the last possibility is to ignore λ, but as can be clearly seen from comparing (27) and (32), this will result in overestimation of the concentration and consequently in underestimation of the brightness.

IG for two component system

To calculate IG for two component system we define seven equations for the factorial cumulants

$$\begin{aligned}K_1&=(\lambda+c_1q_1+c_2q_2)T\\ K_2&=(c_1q_1^2+c_2q_2^2)T^2\\ K_3&=(c_1q_1^3+c_2q_2^3)T^3(2a+2b+3)\frac{64u}{27v^2}\\ K_4&=(c_1q_1^4+c_2q_2^4)T^4(4a+3b+8)\frac{4u^2}{v^3}\\ K_5&=(c_1q_1^5+c_2q_2^5)T^5(10a+6b+25)\frac{4096u^3}{625v^4}\\ K_6&=(c_1q_1^6+c_2q_2^6)T^6(2a+b+6)\frac{4\,096u^4}{27v^5}\\ K_7&=(c_1q_1^7+c_2q_2^7)T^7(14a+6b+49)\frac{8^6u^5}{2\,401v^6}.\end{aligned} \tag{33}$$

System 33 can be solved numerically. However, since high order factorial cumulants are very much affected by noise, the solution is not entirely reliable. Therefore, let us consider some simplifications.

Known background If the background is known, the first equation will take the form $K_1-\lambda T=(c_1 q_1+c_2 q_2)T$ and the last one can be omitted. Such a set of equations can be solved numerically and used for calculation of IG. Still, unstable high order moments are required and additional simplification might be useful.

Known background and instrumental parameters a and b In that case system 22 will take the form

$$\begin{aligned}K_1-\lambda T&=(c_1q_1+c_2q_2)T\\ K_2&=(c_1q_1^2+c_2q_2^2)T^2\\ K_3/\chi_3&=(c_1q_1^3+c_2q_2^3)T^3\\ K_4/\chi_4&=(c_1q_1^4+c_2q_2^4)T^4,\end{aligned} \tag{34}$$

where χ_3 and χ_4 can be calculated from a and b (see 30). System 34 can already be solved analytically (see Appendix 2). In the given approximation, however, it is important to have accurate values for the instrumental parameters a and b. The true parameters a and b are intrinsic to the optical configuration of the instrument used and should be stable from measurement to measurement. So, it is sufficient to accurately fit the first measurement and then to use the obtained parameters a and b as an approximation for the whole experiment. This might be useful for batch processing of data, where

a number of measurements under the same experimental conditions are required.

If no estimates for a and b are available, the following method may be used. The admissible ranges of parameters a and b are subdivided into a number of sections and IG are generated for each section. Finally the set of parameters with the lowest value of χ^2 criterion is accepted. Since IG generation is performed by noniterative calculations it is not time consuming approach.

Testing of the developed algorithm

The common routine of algorithm testing for IG generation includes consecutive tests on noise-free data, then on noisy simulated data, and finally on measured data.

For testing of IG on noisy simulated data several series of PCD with different S/N were generated (50 in each series). The initial value for signal to noise ratio (S/N_i) was taken as the square root of the value at the maximum (this is a simplification, the actual S/N ratio depends on the maximal value of the theoretical PCD and is always higher, see Materials and methods). In each simulated experiment for each PCD IG were calculated, then the obtained IG were combined for calculation of average and standard deviation. The bin time T was 5×10^{-5} s, if not indicated otherwise. If the calculation of IG leads to numerical errors or obtained values are out of acceptable ranges, the simulation was repeated once again in order to achieve 50 PCD in the series.

Testing IG for one component system on simulated data

To evaluate the precision of the numerical model, we have simulated an experiment with noise-free one component PCD, and IG were estimated using (27)–(29). The obtained IG slightly differs from the values, which were used in the simulation. The error originates from the difference in numerical algorithms used for simulation of PCD and calculation of IG. Numerical integration on a finite region and FFT introduce distortions in the simulated PCD. These small systematic errors will also propagate into the factorial cumulants thereby affecting to a greater extent cumulants of higher order. Thus, accuracy of IG depends strongly on the order of used cumulants. In our experiment the relative error was about 0.01% for all parameters except for λ (1.4%). Fixing λ decreases the order of used factorial cumulants to two (27). If, in addition, we fix it to the true value, the relative error for c and q is reduced up to four orders. When λ is fixed, we need only the third and the fourth order cumulants (30) to estimate a and b. Elimination of the fifth order cumulant decreases the error for a and b up to two orders. The relative error for λ is the biggest among the other parameters. A simulation with varying λ shows that the error depends on the difference of λ from the product of c and q. When λ is close to q^*c, the error of λ is of the same order of magnitude as the error for q and it increases with decreasing λ. This is a property of the model, where λ, c and q are essentially interrelated (see 27). It is also obvious that it is hardly possible to estimate background contribution with sufficient accuracy if only a small amount of photons are due to background.

To evaluate the accuracy of IG on noisy simulated PCD several series of PCD with a different S/N ratio were simulated. Results of calculation of IG using (27)–(29) are summarized in Table 1. For high S/N ratio the robustness of IG generation was high enough: less than 2% of simulated PCD leads to physically unacceptable IG, i.e. negative λ or parameters a and b being out of the predetermined admissible bounds. At lower S/N (with S/N_i less than 1,000) about 50% of PCD results in unacceptable combinations of parameters. The clear bias in λ for low S/N is not a property of the tested method; it is a consequence of rejection of negative λ. The same simulation repeated with fixed λ gives significantly better results (see Table 2). No deficient IG were generated even for S/N_i as low as 20. Even for these very low S/N ratios, IG are close to the true values.

In order to test the influence of the background and compare algorithms where λ is free or fixed the IG were estimated from the simulated data with different background levels. The S/N_i was chosen equal to 1,000. According to the first algorithm we estimated all parameters (including λ) using (27)–(29). In the second algorithm, λ was fixed to 1,000 regardless of the value used in for simulations and the other parameters were calculated according to (27) and (30). The results are shown in Table 3. Performed experiments have shown

Table 1 IG calculated for one component PCD simulated with different S/N using (27)–(29) (see Appendix 1 for details)

Parameter	Used for simulation	IG				
		$S/N_I = 7{,}000$	$S/N_i = 5{,}000$	$S/N_i = 3{,}000$	$S/N_i = 1{,}000$	$S/N_i = 500$
c	5	4.994 ± 0.126	4.921 ± 0.145	4.882 ± 0.205	4.327 ± 0.542	4.037 ± 0.728
q	20,000	$20{,}016 \pm 252$	$20{,}165 \pm 298$	$20{,}253 \pm 436$	$21{,}633 \pm 1{,}462$	$22{,}546 \pm 2{,}158$
λ	2,000	$2{,}064 \pm 1{,}260$	$2{,}804 \pm 1{,}459$	$3{,}208 \pm 2{,}086$	$9{,}170 \pm 5{,}948$	$12{,}492 \pm 8{,}267$
a	–1	-0.999 ± 0.019	-0.987 ± 0.023	-0.980 ± 0.034	-0.853 ± 0.152	-0.732 ± 0.274
b	0.5	0.500 ± 0.002	0.499 ± 0.002	0.499 ± 0.003	0.495 ± 0.009	0.503 ± 0.020

If λ becomes negative or parameters a and b exceed the bounds $(-2, 0)$; $(0, 2)$, IG were not included in calculation of average and standard deviations. The clear bias in λ for low S/N is not a property of the tested method; it is a consequence of rejection of negative λ

Table 2 IG calculated for one component PCD simulated with different S/N using (27) and (30) (see Appendix 1 for details)

Parameter	Used for simulation	IG ($\lambda = 1{,}000$)				
		$S/N_i = 1{,}000$	$S/N_i = 500$	$S/N_i = 300$	$S/N_I = 100$	$S/N_i = 50$
c	5	5.000 ± 0.006	4.998 ± 0.016	4.999 ± 0.025	5.005 ± 0.079	4.999 ± 0.107
q	20,000	$20{,}002 \pm 24$	$20{,}008 \pm 69$	$20{,}003 \pm 107$	$19{,}995 \pm 336$	$20{,}029 \pm 455$
a	–1	-1.000 ± 0.004	-1.000 ± 0.008	-1.006 ± 0.015	-1.027 ± 0.051	-1.048 ± 0.106
b	0.5	0.500 ± 0.008	0.502 ± 0.020	0.514 ± 0.033	0.496 ± 0.108	0.522 ± 0.183

λ used for simulation was fixed during the analysis

Table 3 Calculation of IG on simulated data with different level of background according to (27)–(29) (first case: λ is estimated) and (27) and (30) (second case: λ is fixed)

Parameter	Used for simulation	λ	IG				
			$\lambda = 20{,}000$	$\lambda = 10{,}000$	$\lambda = 5{,}000$	$\lambda = 500$	$\lambda = 200$
λ	Varied	Estimated	$19{,}593 \pm 9{,}262$	$14{,}066 \pm 6{,}736$	$9{,}536 \pm 6{,}106$	$8{,}147 \pm 5{,}689$	$7{,}762 \pm 5{,}209$
		Improper IG, (%)	5	20	32	45	60
c	5	Estimated	5.083 ± 0.920	4.623 ± 0.655	4.574 ± 0.571	4.279 ± 0.514	4.287 ± 0.470
		Fixed to 1,000	7.082 ± 0.010	5.942 ± 0.008	5.409 ± 0.007	4.950 ± 0.007	4.921 ± 0.007
q	20,000	Estimated	$20{,}090 \pm 1{,}930$	$20{,}953 \pm 1{,}455$	$21{,}048 \pm 1{,}439$	$21{,}746 \pm 1{,}437$	$21{,}700 \pm 1{,}308$
		Fixed to 1,000	$16{,}804 \pm 25$	$18{,}344 \pm 26$	$19{,}226 \pm 27$	$20{,}100 \pm 29$	$20{,}161 \pm 30$
a	−1	Estimated	-0.976 ± 0.167	-0.915 ± 0.124	-0.906 ± 0.145	-0.839 ± 0.186	-0.848 ± 0.143
		Fixed to 1,000	-1.212 ± 0.005	-1.115 ± 0.005	-1.056 ± 0.004	-0.991 ± 0.004	-0.987 ± 0.004
b	0.5	Estimated	0.503 ± 0.010	0.498 ± 0.008	0.497 ± 0.010	0.497 ± 0.013	0.496 ± 0.007
		Fixed to 1,000	0.527 ± 0.007	0.513 ± 0.009	0.505 ± 0.010	0.496 ± 0.008	0.495 ± 0.008

The percentage of improper IG, with either negative λ or parameters a and b exceeded the bounds $(-2, 0)$; $(0, 2)$, is present. Since no improper IG were calculated for the second case the percentage is given only for the first one. S/N ratio for all simulations was 1,000 and λ was fixed to typical for real measurements value 1 kHz in the second case

that the standard deviations in the second case are independent of the background level used in simulations. The subtraction of λ from the first factorial cumulant does not influence estimation precision but introduces bias, which depends on the difference of λ used in analysis from the actual one. In the case, where λ is free, for the same observation volume, defined by constants a and b, the accuracy of determination of λ increases and the accuracy of c and q decreases with decreasing the difference between λ and $q*c$ (it is evident when the relative errors are compared, data not shown), as it can be expected from the form of (15). This corresponds to the results obtained from the analysis of noise-free data. Finally, the accuracy of parameters a and b does not depend on the difference between λ and $q*c$ as one would expect as well from (15).

To conclude, we recommend using a fixed λ, because it provides robust and accurate estimates without any significant bias for the other parameters. If λ is close to $q*c$, the first approach gives acceptable accuracy for λ and can also be used for IG generation.

Testing IG for a two component system on simulated data

For evaluation of IG for two-component model we simulated a number of PCD with different parameter values and different S/N ratios. IG were estimated using (33). We observed that just for few sets of parameters and an extremely high level of S/N the numerical solution of system 33 (by the Newton–Raphson method) was obtained. The result becomes more robust with fixed λ. Reduction of the order of factorial cumulants by one improved the accuracy and robustness of the calculation and allows practical use for lower S/N ratio. But the numeric solution was still unstable due to poor convergence.

Significantly better results were obtained, when system 34 was used for IG generation. Reduction the order of cumulants to four and the availability of a straightforward noniterative solution (see Appendix 2) improves the accuracy and robustness. Even for low S/N ratios this approach gave correct estimations for concentrations and brightness (see Table 4).

Testing IG for a one component system on measured data

To evaluate the IG generation algorithm on real data we measured Alexa 488 dye. The counting time interval T was chosen at about five times less than the average diffusion time of the measured sample. IG were calculated using (27) and (30) since analysis of simulated data proved that fixing λ gives more accurate and robust IG. Background was estimated from additional measurements of pure solvent. The quality of IG was evaluated

Table 4 IG calculated for two components PCD simulated with different S/N resulted from solution of system 34 (see Appendix 2 for details)

Parameter	Used for simulation	IG			
		$S/N_i = 1{,}000$	$S/N_i = 500$	$S/N_i = 200$	$S/N_i = 100$
c_1	10	9.99 ± 0.13	9.99 ± 0.18	9.86 ± 0.45	10.11 ± 1.70
q_1	20,000	$19{,}883 \pm 635$	$19{,}747 \pm 950$	$19{,}504 \pm 2{,}248$	$18{,}282 \pm 5{,}013$
c_2	2	2.04 ± 0.23	2.07 ± 0.32	2.22 ± 0.75	2.59 ± 1.64
q_2	50,000	$49{,}847 \pm 1{,}404$	$49{,}783 \pm 1{,}802$	$49{,}735 \pm 4{,}562$	$50{,}931 \pm 11{,}676$

χ_3 and χ_4 are calculated using (30). $a = -1$; $b = 0.5$; $\lambda = 1{,}000$; $T = 2\times10^5$ s

Table 5 IG calculated for Alexa 488 using (27) and (30). Best fit parameters and reduced χ^2 criterion are presented for evaluation of quality of IG

Parameters	c	q	a	b	χ^2
IG	24.916	18,500	−1.463	0.321	0.668
Best fit	24.923 ± 0.189	$18{,}500 \pm 141$	-1.472 ± 0.0014	0.324 ± 0.0004	0.666

Confidential intervals for fit parameters were calculated as a square root of diagonal elements of variance–covariance matrix (*ASE*). Background was estimated from additional measurements of pure solvent and fixed to 1.5 kHz. $T = 8\times10^{-6}$ s

by calculation of reduced χ^2 criterion for both obtained sets of parameters. Results of calculations are summarized in Table 5 and shown on Fig. 1a. As it can be clearly seen, estimations are in close agreement with best-fit parameters (residuals calculated for IG and returned from the best fit are almost perfectly overlapped). At the same time, application of (27)–(29) leads to unrealistic, overestimated values for λ and slightly biased estimations of c and q.

An appropriate test of the IG generation algorithm should include some kind of "efficiency evaluation" procedure. It has to estimate robustness of analysis with and without IG and demonstrate higher throughput of analysis based on IG than without IG. To test this a ratio of a number of fit iterations with IG and a number of fit iterations without IG was calculated. In the last case, starting from randomly distributed inside of an admissible range IG, many fit iterations are required, because the number of iterations strongly depends on the proximity of chosen IG to the best fit parameters. Then the number of iterations can be calculated as an average of the number of iterations at each trial. The calculated ratio was 5.1 and the proportion of improper attempts to fit data from random IG (trapping into local minima or failing to fit due to numerical errors) was 48.1% for Alexa 488 (see Table 5).

Testing IG for two component system on measured data

For evaluation of IG for a two-component model on real data a measurement of a mixture of IgG labelled with Alexa 488 and Fab fragment labelled with Cy2 was performed. IG were calculated according to (34). An algorithm consisting of generation of a number of IG for varying a and b, and finally accepting the one with lowest χ^2 was chosen. As the results (Table 6 and Fig. 1b) clearly show, IG are in good agreement with best fit parameters. The accuracy of such a method depends on the step varying both a and b. Thus, one has to find a balance between maximizing the accuracy of IG and minimizing the time of calculations (this was chosen as 0.1 for a and 0.05 for b, respectively, for given IG).

The ratio of a number of fit iterations with and without IG for the given experiment was 8.6 and the

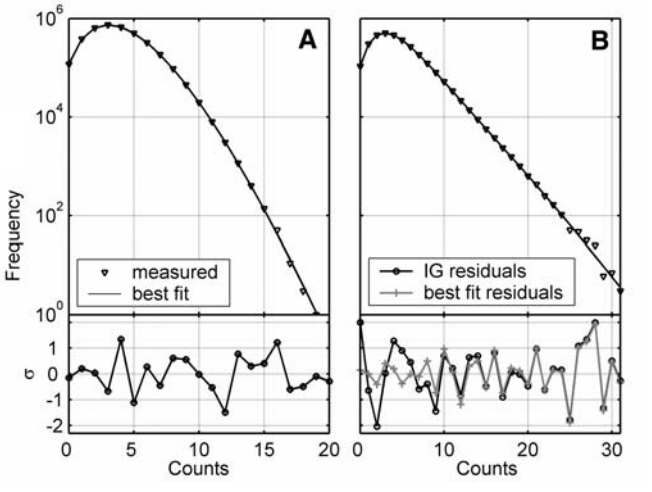

Fig. 1 Best fit of the measured data and superimposed $P(n)$ calculated with IG and correspondent residuals. **a** Best fit and IG of Alexa 488 (see Table 5 for numerical values of parameters). *Theoretical curves* and residuals for both best fit and calculated with IG are almost perfectly overlapped. **b** Best fit and IG of mixture of IgG labeled with Alexa 488 and Fab fragment labeled with Cy2 (see Table 6 for numerical values of parameters). Residuals corresponding to best fit and IG differ slightly at the beginning though *theoretical curves* are almost indistinguishable

Table 6 IG calculated for mixture of IgG labeled with Alexa 488 and Fab fragment labeled with Cy2

Parameters	c_1	q_1	c_2	q_2	a	b	χ^2
IG	5.477	32,099	0.387	90,770	−0.85	0.25	1.26
Best fit	5.166 ± 0.089	32,768 ± 872	0.528 ± 0.052	78,824 ± 2,511	−0.769 ± 0.014	0.296 ± 0.018	0.78

Best fit parameters and reduced χ^2 criterion are presented for evaluation of quality of IG. Confidential intervals for fit parameters were calculated as a square root of diagonal elements of variance–covariance matrix (*ASE*). Background was estimated from additional measurements of pure solvent and fixed to 1.0 kHz. $T = 2\times10^{-5}$ s

proportion of improper fits starting from random IG were 54.5%.

Algorithm of IG generation

Algorithm of IgG generation is summarized in Fig. 2. It consists of rather independent branches for different practical situations, i.e. different number of components, fixing parameters to known values, etc. It's important to emphasizes once more, the accuracy of IG depends on order of used cumulants and therefore in each particular case one has to try to find solution using cumulants of possibly minimal order.

Minima in χ^2 criterion surface

Any theoretical model must be fully identifiable, i.e. a unique set of parameters must describe particular data in the best way, or in other words only one global minimum must exist. However, this is not the case for FIDA.

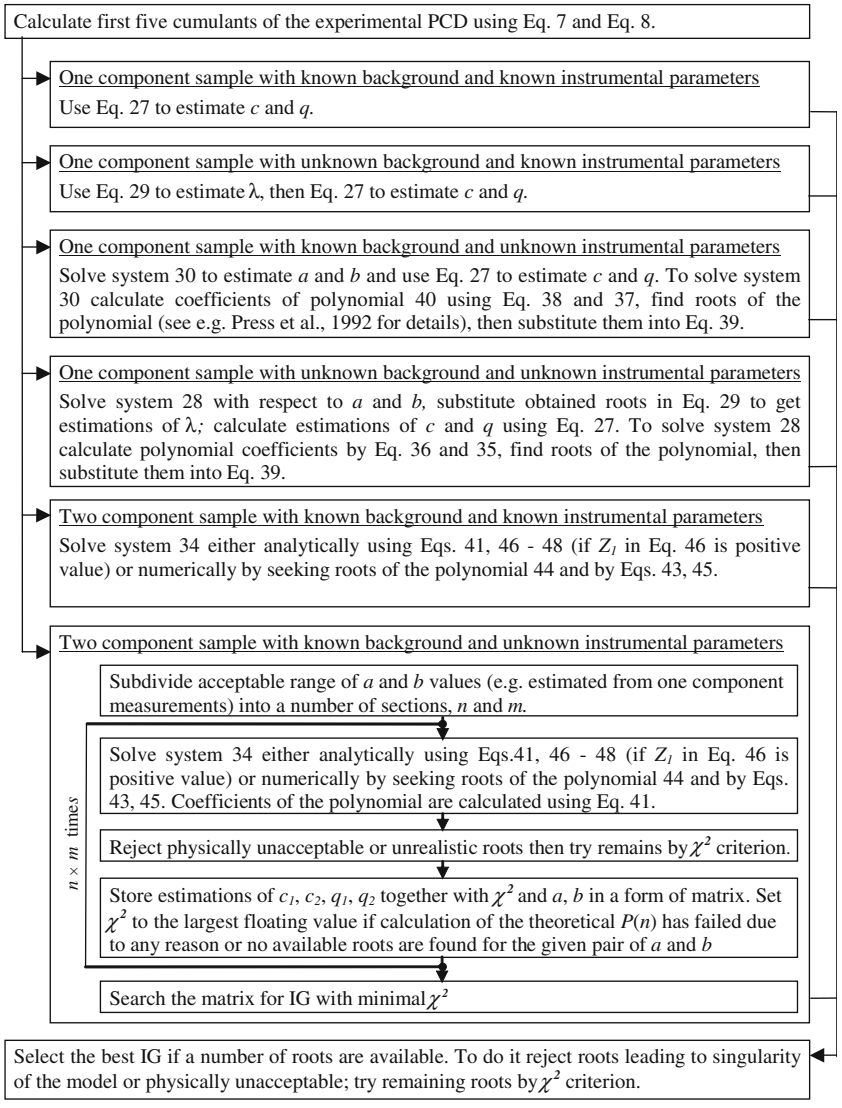

Fig. 2 Algorithm of IG generation for FIDA

The existence of at least three minima related to different pairs of a and b (with fixingλ) was predicted theoretically. Fortunately, unique values for physically meaningful parameters c and q hold for all possible combinations of a and b. As a and b are artificial parameters introduced for the best approximation of the actual observation profile (all possible combinations of a and b generate precisely the same values for geometrical factors χ_k), the existence of several minima should not be considered as a weak point of FIDA. For visualization, the χ^2 criterion was calculated varying both a and b. Figure 3 shows a surface of χ^2 plotted versus a and b (c and q were fixed to values obtained from the best fit, Table 5). There are three distinct minima in the plot, separated by a plane where χ^2 goes to infinity. Indeed the solution of system 30 gives three pairs of a and b (see Table 7). The inspection of the χ^2 surface validates values shown in Table 7 as possible minima in the surface. The existence of discontinuity points is evident from (30): all geometrical factors χ_k tend to infinity when a and b satisfy equation $2a+3b+2=0$. Thus, the situation is created by chosen normalization conditions in form of (14) and makes the analysis more complicated because of possible trapping into break point (or close to it) from iteration to iteration.

Calculation of χ^2 has shown that there are minor differences in χ^2 criterion for those sets of parameters (theoretically they must be the same). Because q and c are calculated independently from a and b and remain the same and both three pairs of a and b gives the same values for χ_k, the difference may originate from inaccuracy in numerical calculation of PCD. Test on noise-free simulated PCD have shown that very small deviation in calculation of χ^2 still present and thus originated primarily from inaccuracy in numerical calculation.

In our calculations we often observe the values of the χ^2 criterion lower then 1. The low number of the degrees of freedom in χ^2 criterion is probably responsible for that effect. Typically, the number of nonzero PCD channels (actually used in χ^2 calculation) is less then 20,

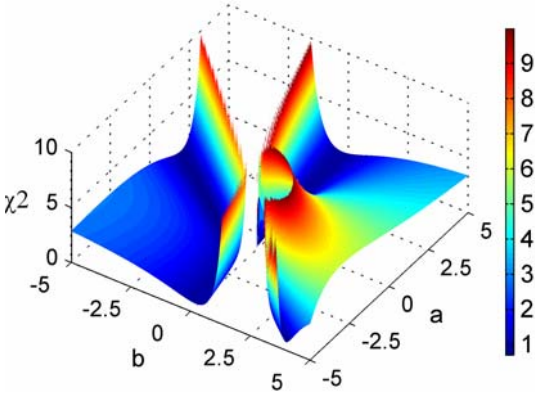

Fig. 3 Surface of χ^2 plotted versus brightness profile parameters a and b. c and q were kept equal to best fit values of Alexa 488 (see Table 5). There are three distinct minima on the graph (see Table 7 for numerical values) that are separated by a plain where χ^2 goes to infinity

Table 7 Solution of system 30 for Alexa 488 (see Table 5). Three pairs of parameters a and b, which ensures a comparable quality of fit, are available

Parameters	Set 1	Set 2	Set 3
a	−1.393	−1.463	−4.643
b	−0.861	0.321	3.539
χ^2	0.732	0.668	0.711

which leads to essentially skewed χ^2 distribution. To illustrate that, we calculated χ^2 criterion for 1,000 simulated PCD differing in noise realization. The resulted histogram of χ^2 values is presented in Fig. 4. Though the χ^2 values are distributed around unity with the average 1.007, almost 30% of values are well below 0.9 (the lowest value is 0.34!). Thus, χ^2values below unity are just a result of probable fluctuation from expected average value, i.e. unity, and do not provide any additional proofs the fit quality. The standard deviations of χ^2 distribution and consequently the probability to obtain χ^2 lower then unity decrease, as the number of degrees of freedom in χ^2 criterion increases.

Discussion

Here we propose an effective method of IG generation for FIDA. The test experiments demonstrated that correct estimates are obtained not only for brightness and concentration, but also for background and brightness profile parameters. Since we have the estimates for all model parameters and in the most cases they are in close proximity to the best fit parameters, the iterative procedure started from those estimates goes to the global minima in just a few iterations. This in turn

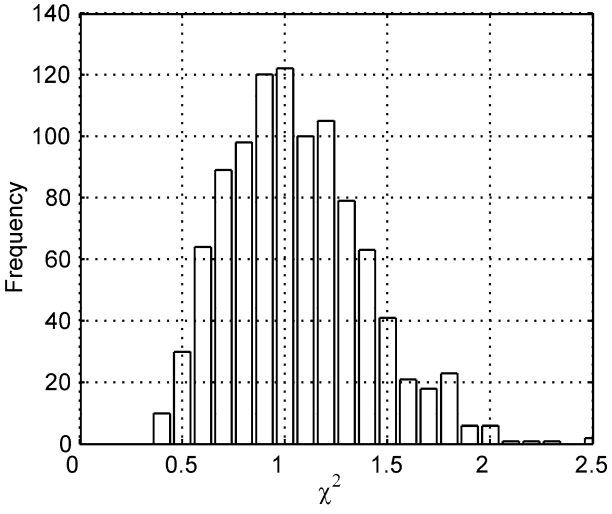

Fig. 4 Histogram of χ^2 values for 1,000 simulated PCD differing only in noise realization. Parameters of the simulated PCD were kept as close as possible to reproduce measured PCD of Alexa 488 (see Table 5). Though the χ^2 values are distributed about unity with the average 1.007, almost 30% of values are below 0.9

increases the speed and throughput of the analysis. Moreover we showed that application of IG reduces the probability of crashes due to numerical errors (division by zero, overflows of exponential, etc) and obtaining parameters outside the model domain by almost 50%.

Still, the developed algorithm has a few limitations. Although the method of moments can deliver the estimates for all parameters of a molecular system with n-components, instability of high order factorial cumulants of PCD puts rather strict limits on its practical performance. We found that good results were obtained using the first five cumulants. Higher cumulants may not only distort the estimates but also very often lead to the divergence of the numerical solution. Thus, IG for only one and two component models can be calculated with sufficient accuracy. One could extend the calculations for three or even more component system, but practically we are most likely restricted to a two component system, which anyway covers most of the current applications. Analysis of simulated data has shown, that it is possible to find an appropriate IG for a three component system, but the robustness of the calculations was quite poor. In addition, normalization conditions chosen for FIDA imply the existence of discontinuity points in the model domain. It makes the analysis more complicated because of possible trapping into break point or close to it from iteration to iteration.

Finally, one interesting feature revealed in the detailed mathematical analysis of FIDA model should be emphasized. The model of observation profile and normalization conditions assumed in FIDA implies the existence of three sets of parameters for one component model, which may be used as IG. If the background is fixed, all three sets of parameters ensure a comparable quality of the fit. All obtained combination of parameters are acceptable and the χ^2 criterion cannot help to choose the best one. Analysis of a large amount of simulated and measured data has shown that pairs of a and b differ much in their values. For example one pair has both negative values and another one, though having opposite signs, differs in values in several times. Taking into account that a and b are instrumentation parameters and are more or less stable from measurement to measurement, one can set the reasonable margins and use them for the roots selection. Existence of discontinuity points in model domain and a number of possible minima requires further comprehensive numerical and statistical analysis of the FIDA model.

Besides generation of the IG the proposed method can also be used independently for estimation of brightness and concentrations of measured samples with sufficient accuracy. However, the method of moments itself gives no insight in the statistical quality of data (Muller 2004). Therefore we invested so much time in evaluation of applicability and limitations of this method. And finally, the application of our algorithm is not limited by FIDA, but with minor changes it might be implemented in PCH and FCA.

Appendix 1

System 28 can be written in the following way

$$\begin{cases} a^2(16u-20)+b^2(9u-12)+8ab(3u-4) \\ \quad +16a(4u-5)+b(48u-68)+(64u-75)=0 \\ a^2(4v-8)+b^2(4v-9)+2ab(4v-9)+12a(v-2) \\ \quad +b(12v-30)+(9v-16)=0, \end{cases} \tag{35}$$

where

$$u=\frac{16\,875K_5K_3}{16\,384K_4^2}, \quad v=\frac{1\,024K_4K_2}{729K_3^2}. \tag{36}$$

Similarly, for system 30

$$\begin{cases} 4a^2(u-1)+3b^2(3u-4)+4ab(3u-4)+8a(u-1)+ \\ \quad 4b(3u-5)+(4u-3)=0 \\ a^2(4v-8)+b^2(6v-18)+ab(10v-30)+a(10v-20)+ \\ \quad b(13v-51)+(6v-8)=0, \end{cases} \tag{37}$$

where

$$u=\frac{27K_3(K_1-\lambda T)}{64K_2^2}, \quad v=\frac{16K_4(K_1-\lambda T)}{27K_2K_3}. \tag{38}$$

The both systems 35 and 37 can be reduced to a fourth order polynomial and solved either analytically or numerically. Denote factors after a^2, b^2, ab,a,b,1 in system 35 (derivation is also valid for system 37) as A_1-A_6 (first equation) and B_1-B_6 (second equation) consequently. Combining equations from system 35 leads to the estimate for b

$$b=-\frac{D_1a^2+D_3a+D_5}{D_2a+D_4}, \tag{39}$$

where $D_1=A_1\,B_2-A_2\,B_1$, $D_2=A_3\,B_2-A_2\,B_3$, $D_3=A_4\,B_2-A_2\,B_4$, $D_4=A_5\,B_2-A_2\,B_5$, $D_5=A_6\,B_2-A_2\,B_6$. Substitution (39) into second equation of system 35 yields the fourth order polynomial

$$\begin{aligned} &(B_1D_1^2+B_2D_1^2-B_3D_1D_2)a^4 \\ &+(2B_1D_2D_4+2B_2D_1D_3-B_3D_1D_4-B_3D_2D_3+ \\ &B_4D_2^2-B_5D_1D_2)a^3 \\ &+(B_1D_4^2+B_2D_3^2+2B_2D_1D_5-B_3D_3D_4-B_3D_2D_5 \\ &+2B_4D_2D_4-B_5D_1D_4-B_5D_2D_3+B_6D_2^2)a^2 \\ &+(2B_2D_3D_5-B_3D_4D_5+B_4D_4^2-B_5D_3D_4-B_5D_2D_5 \\ &+2B_6D_2D_4)a \\ &+(B_2D_5^2-B_5D_4D_5+B_6D_4^2)=0. \end{aligned} \tag{40}$$

If the discriminant of the polynomial is positive value, a real valued analytical solution is available for a. There are two real and two complex-conjugate roots in that case (Korn and Korn 1968). One real root (always represented by values $a=-7/2$ and $b=2$) leads to singularity of the model and must be omitted. If discriminant is negative, four real roots are available and numerical algorithms are required to evaluate the roots of the polynomial.

Appendix 2

System 34 can be reduced to third order polynomial and solved either analytically or numerically. Denote left hand parts in system 34 as

$$\begin{cases} (K_1-\lambda T)/T=A_1 \\ K_2/T^2=A_2 \\ 27(2a+3b+2)^2K_3/64(2a+2b+3)(2a+6b+1)T^3=A_3 \\ (2a+3b+2)^3K_4/4(4a+3b+8)(2a+6b+1)^2T^4=A_4. \end{cases} \tag{41}$$

After reducing system 34 with respect to q_1 we arrive at

$$\begin{cases} A_2c_2q_2^4-2A_3c_2q_2^3+A_2c_2q_2^2-A_2A_4+A_3^2=0 \\ A_1c_2q_2^4-A_2c_2q_2^3-A_3c_2q_2^2+A_4c_2q_2-A_1A_4+A_2A_3=0. \end{cases} \tag{42}$$

From first equation we get expression for c_2

$$c_2=\frac{A_2A_4-A_3^2}{A_2q_2^4-2A_3q_2^3+A_4q_2^2} \tag{43}$$

and after substitution (43) into second equation of system 42 we arrive at third order polynomial

$$\begin{aligned}&(A_2^3A_3-A_3^2A_1)q_2^3+(2A_1A_3A_4-A_2^2A_4-A_2A_3^2)q_2^2 \\ &+(A_3^3-A_1A_4^2)q_2+(A_4^2A_2-A_3^2A_4)=0.\end{aligned} \tag{44}$$

Finally

$$q_1=\frac{A_3-c_2q_2^3}{A_2-c_2q_2^2},\quad c_1=\frac{A_1-c_2q_2}{q_1}. \tag{45}$$

If the discriminant of the polynomial is positive value, a real valued analytical solution is available (it can be easily obtained by using symbolic toolbox in Matlab (http://www.mathworks.com) or Mathcad (http://www.mathcad.com). If we denote

$$\begin{aligned} Z_1&=A_4^2A_1^2-6A_1A_2A_3A_4-3A_3^2A_2^2+4A_1A_3^3+4A_4A_2^3 \\ Z_2&=A_1^3A_4^2+A_1^3A_3(2A_3^2-5A_2A_4)+3A_1A_4A_2^3-A_3A_2^4 \\ Z_3&=A_1^2A_4-2A_1A_2A_3+A_2^3 \end{aligned} \tag{46}$$

then

$$q_1=\frac{\sqrt{Z_1}-A_1A_4+A_2A_3}{2(A_2^2-A_1A_3)},\quad q_2=\frac{\sqrt{Z_1}+A_1A_4-A_2A_3}{2(A_1A_3-A_2^2)} \tag{47}$$

$$c_1=\frac{\sqrt{Z_1}Z_2+Z_1Z_3}{2Z_1(A_2A_4-A_3^2)},\quad c_2=\frac{\sqrt{Z_1}Z_2-Z_1Z_3}{2Z_1(A_3^2-A_2A_4)}. \tag{48}$$

If the discriminant of the polynomial is negative, two or three real roots are available. They can be found by the numerical seeking roots of the polynomial.

References

Chen Y, Müller JD, So PT, Gratton E (1999) The photon counting histogram in fluorescence fluctuation spectroscopy. Biophys J 77:553–567

Chen Y, Müller JD, Tetin SY, Tyner JD, Gratton E (2000) Probing ligand protein binding equilibria with fluorescence fluctuation spectroscopy. Biophys J 79:1074–1084

Chen Y, Müller JD, Ruan Q, Gratton E (2002) Molecular brightness characterization of EGFP in vivo by fluorescence fluctuation spectroscopy. Biophys J 82:133–144

Deelder AM, van Dam GJ, Kornelis D, Fillie YE, van Zeyl RJ (1996) Schistosoma: analysis of monoclonal antibodies reactive with the circulating antigens CAA and CCA. Parasitology 112(Pt 1):21–35

Demas JN (1983) Exited state lifetime measurements. Academic Press, New York

Elson EL, Magde D (1974) Fluorescence correlation spectroscopy. I. Conceptual basis and theory. Biopolymers 13:1–27

Evotec Biosystems AG (1998) International Patent Application PCT/EP97/05619 and International Publication No. WO 98/16814

Hess ST, Huang S, Heikal AA, Webb WW (2002) Biological and chemical applications of fluorescence correlation spectroscopy: a review. Biochemistry 41:697–705

Johnson LM, Faunt LM (1992) Parameter estimation by least–squares methods. Methods Enzymol 210:1–37

Kask P, Palo K, Ullmann D, Gall K (1999) Fluorescence-intensity distribution analysis and its application in biomolecular detection technology. Proc Natl Acad Sci USA 96:13756–13761

Kask P, Palo K, Fay N, Brand L, Mets Ü, Ullmann D, Jungmann J, Pschorr J, Gall K (2000) Two-dimensional fluorescence intensity distribution analysis: theory and applications. Biophys J 78:1703–1713

Kask P, Eggeling C, Palo K, Ullmann D, Gall K (2002) Fluorescence intensity distribution analysis (FIDA) and related fluorescence fluctuation techniques: theory and practice. In: Kraayenhof R, Visser AJWG, Gerritsen HC (eds) Fluorescent spectroscopy, imaging and probes. New tools in chemical, physical and life sciences. Springer-Verlag, Berlin Heidelberg, pp 153–181

Koppel DE (1974) Statistical accuracy in fluorescence correlation spectroscopy. Phys Rev A 10(N6):1938–1945

Korn GA, Korn TM (1968) Mathematical handbook for scientists and engineers. Definitions, theorems and formulas for reference and review. Second, enlarged and revised edition. McGraw-Hill Book Company, New York

Lau HT (1995) A numerical library in C for scientists and engineers. CRC Press Inc., Boca Raton

Magde D, Elson EL, Webb WW (1972) Thermodynamic fluctuations in a reacting system: measurement by fluorescence correlation spectroscopy. Phys Rev Lett 29:704–708

Magde D, Elson EL, Webb WW (1974) Fluorescence correlation spectroscopy. II. An experimental realization. Biopolymers 13:29–61

Marquardt DW (1963) Algorithm for least squares estimation of nonlinear parameters. J Soc Ind Appl Math 11:431–441

Meseth U, Wohland T, Rigler R, Vogel H (1999) Resolution of fluorescence correlation measurements. Biophys J 76:1619–1631

Müller JD (2004) Cumulant analysis in fluctuation spectroscopy. Biophys J 86:3981–3992

Müller JD, Chen Y, Gratton E (2000) Resolving heterogeneity on the single molecular level with the photon counting histogram. Biophys J 78:474–486

Palo K, Mets Ü, Jager S, Kask P, Gall K (2000) Fluorescence intensity multiple distribution analysis: concurrent determination of diffusion times and molecular brightness. Biophys J 79:2858–2866

Palo K, Brandt L, Eggeling C, Jager S, Kask P, Gall K (2002) Fluorescence intensity and lifetime distribution analysis: toward higher accuracy in fluorescence fluctuation spectroscopy. Biophys J 83:605–618

Press WH, Teukolsky SA, Vetterling WT, Flannery BP (1992) Numerical recipes in C. The art of scientific computing. 2nd edn. Cambridge University Press, Cambridge

Qian H (1990) On the statistics of fluorescence correlation spectroscopy. Biophys Chem 38:49–57

Qian H, Elson EL (1990a) On the analysis of high order moments of fluorescence fluctuations. Biophys J 57:375–380

Qian H, Elson EL (1990b) Distribution of molecular aggregation by analysis of fluctuation moments. Proc Natl Acad Sci USA 87:5479–5483

Remoortere A, Hokke CH, van Dam GJ, van Dam I, Deelder AM, van den Eijnden DH (2000) Various stages of schistosoma express Lewis(x), LacdiNAc, GalNAcbeta1-4 (Fucalpha1-3)GlcNAc and GalNAcbeta1-4(Fucalpha1-2Fucalpha1-3)GlcNAc carbohydrate epitopes: detection with monoclonal antibodies that are characterized by enzymatically synthesized neoglycoproteins. Glycobiology 10:601–609

Rigler R, Mets Ü, Widengren J, Kask P (1993) Fluorescence correlation spectroscopy with high count rates and low background: analysis of translational diffusion. Eur Biophys J 22:169–175